Electronic states and local structures of the photomagnetic Cu-Mo cyanides $Cu_2Mo(CN)_8 \cdot 8H_2O$ and $Cs_{0.5}Cu_{1.75}Mo(CN)_8 \cdot 1.5H_2O$ studied by x-ray absorption fine structure spectroscopy

Xiao-Dong Ma,[1] Toshihiko Yokoyama,[1,2,*] Toshiya Hozumi,[3] Kazuhito Hashimoto,[3] and Shin-ichi Ohkoshi[3,4]
[1]*Department of Structural Molecular Science, Graduate University of Advanced Studies (Sokendai), Myodaiji-cho, Okazaki, Aichi 444-8585, Japan*
[2]*Institute for Molecular Science, Myodaiji-cho, Okazaki, Aichi 444-8585, Japan*
[3]*Department of Applied Chemistry, Graduate School of Engineering, The University of Tokyo, 7-3-1 Hongo, Bunkyo-ku, Tokyo 113-8656, Japan*
[4]*PRESTO, JST, 4-1-8 Honcho, Kawaguchi, Saitama 332-0012, Japan*
(Received 13 March 2005; revised manuscript received 17 June 2005; published 13 September 2005)

The electronic states and local structures of photomagnetic CuMo cyanides, $Cu_2Mo(CN)_8 \cdot H_2O$ and $Cs_{0.5}Cu_{1.75}Mo(CN)_8 \cdot 1.5H_2O$, have been studied by Cu and Mo *K*-edge x-ray-absorption fine-structure spectroscopy. A direct evidence for the reduction of divalent Cu to monovalent is detected by Cu *K*-edge x-ray-absorption near-edge structure. The extended x-ray-absorption fine-structure confirms that the interatomic distances around Cu and Mo in the photoinduced phase are almost identical to those of the initial low-temperature phase. The higher-nearest neighbor coordination numbers, however, are apparently reduced. We have interpreted this as the result of the bending of the Mo-CN bond due to the tetrahedral distortion around the Cu(I) site.

DOI: 10.1103/PhysRevB.72.094107 PACS number(s): 61.10.Ht, 75.30.Kz, 75.50.−y, 75.50.Dd

I. INTRODUCTION

Prussian-blue analogs often exhibit noble magnetic properties such as photoinduced magnetization[1,2] and high Curie temperature.[3,4] The photoinduced magnetization involves a charge transfer, which results in a change in the metal spin states during light irradiation. Structure information regarding the photoinduced magnetization is extremely important to understand the magnetic properties. The single-crystal x-ray diffraction technique is, however, hardly applicable to the Prussian-blue analogs since usually the samples can only be obtained as a fine powder. Even if a single crystal is obtained, the photoexcitation experiment for a single crystal is not easily performed since it is difficult to excite a whole crystal uniformly. In such a case, extended x-ray-absorption fine-structure (EXAFS) spectroscopy is useful to obtain information on local structures around transition metal atoms. Moreover, x-ray absorption near-edge structure (XANES) spectra provide information on electronic states. The x-ray-absorption fine-structure (XAFS) studies on photomagnetic Prussian-blue analogs have been performed for CoFe,[5–7] CoW,[8] and MnFe (Ref. 9) cyanides.

CuMo cyanides have also been attractive photomagnets. $Cu_2Mo(CN)_8 \cdot H_2O$ (1) undergoes a photoinduced phase transition at low temperature (LT) with a Curie temperature of 17 K.[10–13] It is believed that a charge transfer occurs from Mo(IV) to Cu(II) and that the resultant photoinduced phase consists of Cu(I) and Mo(V). Very recently, a type of the CuMo cyanide, $Cs_{0.5}Cu_{1.75}Mo(CN)_8 \cdot 1.5H_2O$ (2), has been successfully synthesized by Hozumi *et al.*[14] They have found several noble properties in this compound. A photomagnetic property was found with a higher Curie temperature of 23 K. Since the compound is prepared electrochemically, transparent thin films with desired uniform thicknesses can be obtained much more easily than with a fine powder. Moreover, they have succeeded in the growth of single crystals and have performed the crystal structure determination before the photoirradiation.

In the present work, we have investigated the local structures and the electronic states mainly of the photoinduced phases of these two CuMo cyanides by means of the XAFS technique. Although our research group has already performed several XAFS studies on Prussian-blue analogs, the present investigation is still important for the following reasons. First, the photoinduced phase is an essentially different state for these compounds. Usually, the photoinduced phase at low temperature (LT) is considered to be structurally identical to that of the corresponding high-temperature (HT) phase. The CuMo cyanides are, however, in the LT phase even at room temperature and are likely to decompose with the temperature rise before the thermally driven phase transition takes place. Second, these compounds, which show ferromagnetism, consist only of magnetic ions of Cu and Mo, which seldom exhibit ordered magnetism. No typical magnetic ions such as Mn, Fe, Co, or Ni are present. Third, the change of local structures around Cu in a redox cycle is an important issue in various scientific fields such as catalysis and biology. In the CuMo cyanides, a reduction of Cu from divalent to monovalent is expected on the photoirradiation as in the previous cases of the CoFe, CoW, and MnFe cyanides. In the previous examples, however, significant changes in the interatomic distances occurred. On the contrary, only a slight or negligible change in the interatomic distance is expected in the reduction of Cu. Instead, there have been several known structural models, although in some materials there still remains controversy. In divalent Cu, square planar coordination with four ligands is usually most stable, while in monovalent Cu, trigonal pyramid with three ligands, tetrahedron with four ligands, and square pyramid with five ligands are known. The changes of the local

structure around Cu is thus interesting also in the present CuMo cyanides.

In this paper, we will first present the Cu *K*-edge XANES spectra during photoirradiation and will give direct proof that Cu is gradually reduced. Subsequent EXAFS analysis reveals the local structures of the photoinduced phases of the CuMo cyanides (1) and (2) as well as of the initial ground states. Finally, we will present a possible model of the local structure changes around Cu upon photoirradiation.

II. EXPERIMENTS

Samples (1) and (2) were synthesized according to the literature.[10,14] For sample (2), a favorable thin film (~500 nm thick) was prepared electrochemically on a SnO_2-coated glass substrate. A reference material of $[Cu(cyclam)]_2[Mo(CN)_8]10.5\cdot H_2O$ (3) (*cyclam*=1,4,8,11-tetraazacyclodecane) was also prepared in a reported method.[15]

The XAFS measurements were performed at Beamlines 10B and 12C of the Photon Factory at High Energy Accelerator Research Organization (KEK-PF) (Tsukuba, Japan). The storage ring was operated with the electron energy of 2.5 GeV and the ring current of 400–250 mA. At Beamline 10B, transmission XAFS spectra were taken for Cu and Mo *K* edges of (1), (2), and (3) at 30 K. Mo *K*-edge XAFS spectra of $Cs_3Mo(CN)_8\cdot H_2O$ (4) were also recorded. A Si(311) channel-cut crystal monochromator was employed. Higher-order harmonics were less important in the operation of the ring energy of 2.5 GeV. Incident (I_0) and transmitted (I) x-ray intensities were simultaneously measured with ionization chambers (lengths of 17 cm for I_0 and 31 cm for I) filled with appropriate gases: N_2 100% (I_0) and N_2 50%/Ar 50% (I) for the Cu *K* edge and N_2 50%/Ar 50% (I_0) and Ar 100% (I) for the Mo *K* edge.

At Beamline 12C, fluorescence XAFS spectra were taken for (1) and (2) at 30 K. Fluorescence detection was essential to measure XAFS of the photoinduced phase because the penetration depth of the visible light is much smaller than that of the x rays and the appropriate thickness of the sample is too thin to record transmission XAFS spectra. A thin film of (2) was used as it was. On the other hand, sample (1) was obtained as a fine powder, and a thin film was produced by dispersing powder on an adhesive tape uniformly so as to make it as transparent as possible. A Si(111) double crystal monochromator was employed and detuned slightly (~80%) in order to reduce higher-order harmonics. The incident x-ray intensity (I_0) was measured with an ionization chamber filled with N_2 100% for the Cu *K* edge and N_2 50%/Ar 50% (I) for the Mo *K* edge. The fluorescence x-ray intensity was also detected with an ionization chamber filled with Ar for both edges. In order to record the XAFS spectra of the photoinduced phases, the samples were irradiated by blue light from a solid state laser (473 nm) for 30–60 min. During the laser irradiation, continuous XANES measurements were performed.

III. RESULTS AND DISCUSSION

Figure 1(a) shows the Cu *K*-edge XANES of (1) and (2) before and after photoirradiation, together with the reference

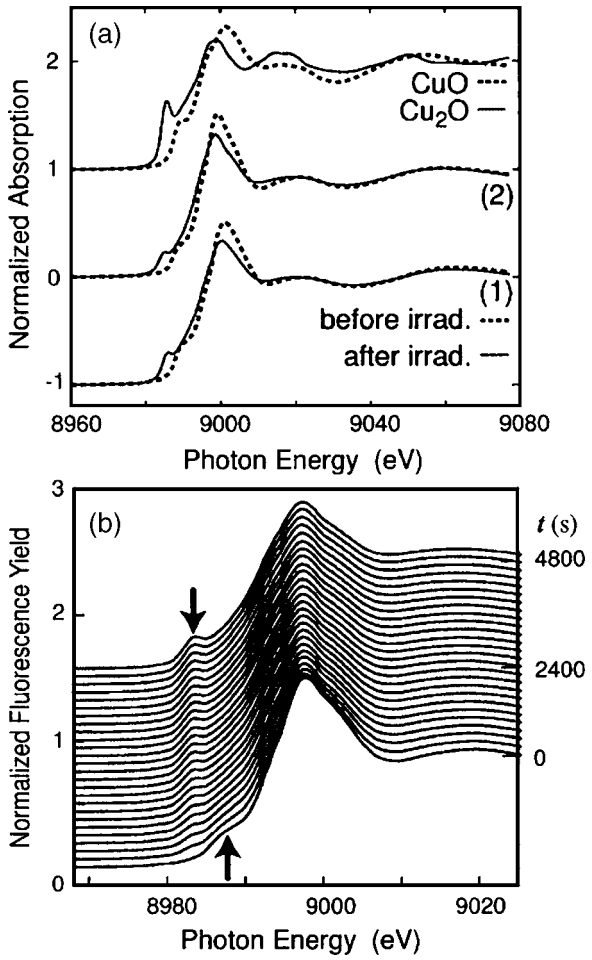

FIG. 1. (a) Cu *K*-edge XANES of (1) (bottom) and (2) (middle), together with Cu_2O and CuO (top). (b) Time evolution of Cu *K*-edge XANES of (2) during laser irradiation.

spectra of CuO and Cu_2O. As illustrated in the reference spectra, monovalent Cu shows a typical resonance peak at ~8984 eV, while divalent Cu gives a weak $1s\rightarrow 3d$ absorption at ~8981 eV and a shoulder at ~8990 eV. One can immediately conclude that Cu(II) in (1) and (2) is reduced to Cu(I) after photoirradiation. This is the first direct proof that the charge transfer actually occurs in the photoinduced phase transition of the CuMo cyanide. Figure 1(b) gives the time evolution of Cu *K*-edge XANES of (2) during photoirradiation. It shows that the typical shoulder for Cu(II) is apparently weakened, while the one for Cu(I) is increased during irradiation. It is noted that when the intensities of the peaks at 8984 and 8990 eV are plotted logarithmically, linear kinetics of the present photoreaction is suggested (not shown), and the saturation of the reaction was also confirmed.

Figure 2 shows the Mo and Cu *K*-edge EXAFS oscillation functions $k^3\chi(k)$ and their Fourier transforms (FT) of (1–4) taken in the transmission mode. The EXAFS functions were obtained by standard procedures as the subtraction of the preedge baseline and the postedge background (cubic spline functions), followed by normalization using the atomic absorption coefficients. For assignments of the features in the FTs, let us briefly summarize structural information reported previously.[13–16] In all samples of (1–4), there exist $Mo(CN)_8$

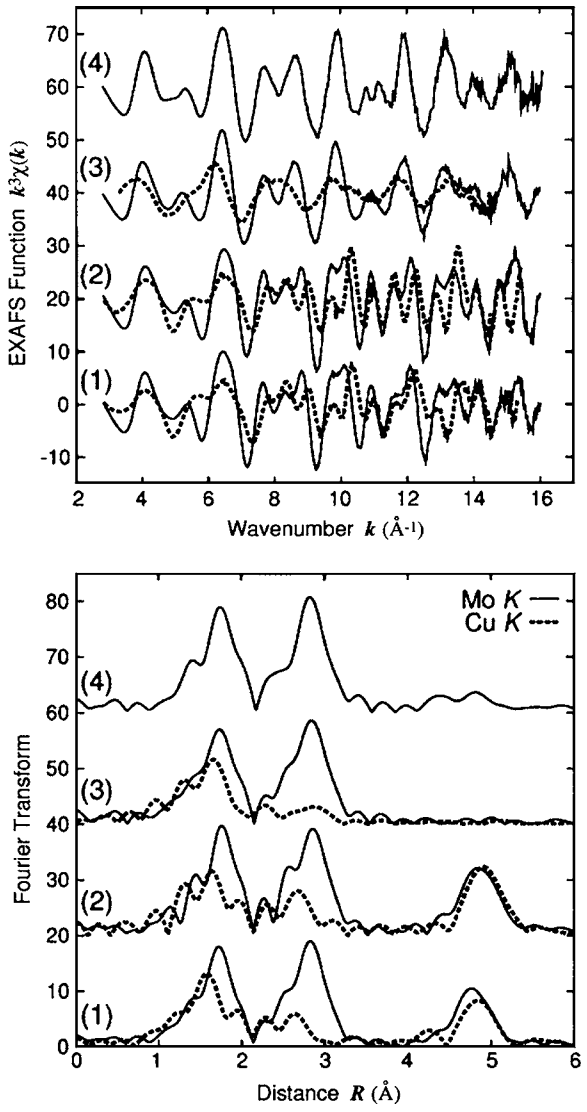

FIG. 2. Mo and Cu K-edge EXAFS oscillation functions $k^3\chi(k)$ and the Fourier transforms of (1–4) at 30 K taken in the transmission mode.

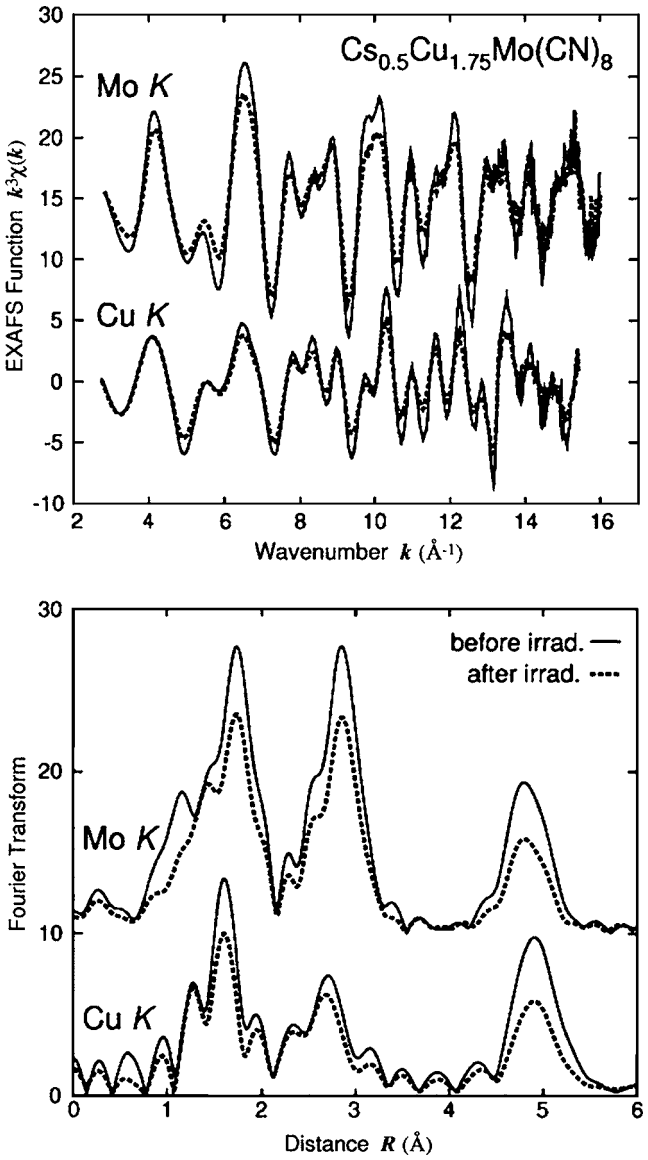

FIG. 3. Mo and Cu K-edge EXAFS oscillation functions $k^3\chi(k)$ and the Fourier transforms of (2) at 30 K before and after laser irradiation.

units, and in (1–3) the $Mo(CN)_8^{4-}$ unit is linked to Cu. In (1),[13] Cu is surrounded by four equatorial NC^- and two axial H_2O. On the other hand, in (2),[14] there exist two inequivalent Cu with the composition ratio of Cu1:Cu2=4:3. Cu1 shows square pyramidal coordination consisting of four equatorial and one axial NC^-, while Cu2 exhibits similar structure to that in (1).

In all of the FTs of the Mo K-edge EXAFS, contributions of the Mo-C (~1.7 Å) and Mo-N (~2.9 Å) shells are clearly seen, while in the FTs of (1) and (2), additional contributions are found at ~4.8 Å, which can be assigned to the Mo-Cu shell. The fact that the Mo-N and Mo-Cu shells appear prominently in the FTs implies essential collinearity of the Mo-CN-Cu configuration. Although sample (4) also shows some weak contributions around 4.0–5.3 Å, these features can be ascribed to Cs contribution.[16] On the other hand, in the FTs of the Cu K-edge EXAFS of (1) and (2), contributions of the Cu-N (~1.6 Å), Cu-C (~2.7 Å), and Cu-Mo shell (~5.0 Å) are observable. On the contrary, in the FTs of (3), the corresponding Cu-C shell is quite weak and the Cu-Mo shell is completely missing. This is because the Cu-N-C angle is strongly bent (~145°) and the multiple-scattering focusing effect is not important. Figure 3 shows the Mo and Cu K-edge EXAFS functions $k^3\chi(k)$ and the FTs of (2) before and after photoirradiation, taken in the fluorescence yield mode. The EXAFS oscillations are quite similar between the LT and photoinduced phases, although the EXAFS amplitude is noticeably reduced after photoirradiation.

Curve-fitting analysis was performed for each contribution in k space. In order to obtain the backscattering amplitudes and the phase shifts, we have performed theoretical simulations using the FEFF (version 8.00) (Ref. 17) code for (2–4) based on the reported crystal structures.[14–16] Since the Mo-C-N-Cu configuration is nearly collinear, the EXAFS function of the higher-nearest neighbor (NN) shells such as

TABLE I. The interatomic distances (Å unit) from the Mo *K*-edge EXAFS analysis of (1–4). PI denotes the photoinduced state. The errors are given in parentheses, which apply to the last digit.

Sample	Reference	Mo-C	Mo-N	Mo-Cu
(1)LT	This work	2.155(2)	3.306(2)	5.233(5)
(1)PI	This work	2.152(3)	3.299(3)	5.217(10)
(2)LT	This work	2.159(3)	3.310(2)	5.256(4)
	14	2.157	3.305	5.240
(2)PI	This work	2.158(3)	3.308(3)	5.257(6)
(3)LT	This work	2.168(3)	3.326(2)	
	15	2.157	3.319	
(4)LT	This work	2.171(2)	3.311(2)	
	16	2.171	3.310	

Mo-N, Mo-Cu, Cu-C, and Cu-Mo should be given as a sum of all the corresponding single- and multiple-scattering components.[18–21] By summing up all the components, the one-shell analysis can be performed as in the first-NN single-scattering cases. This simplification is physically valid when the Mo-C-N-Cu configuration is nearly collinear. This is because the interatomic distances and the Debye-Waller factors are all equal among these single- and multiple-scattering paths, as long as the dynamic effect mainly due to the bending vibration does not contribute so much to the reduction of the backscattering amplitudes.[22–24] Moreover, this simplification is mathematically valid even for noncollinear cases, although the interatomic distance and the Debye-Waller factor are not identical for each scattering path and the Debye-Waller factor obtained from the analysis corresponds to some average and is less physically meaningful. These treatments for the multiple-scattering paths are identical to our previous data analysis.[5,6,8,9]

In the FTs of the Mo *K*-edge EXAFS (typical *k* range employed was 2.7–16.0 $Å^{-1}$), the three shells of Mo-C, Mo-N, and Mo-Cu are well separated from each other, and thus the single-shell analysis could be done. The *R* and *k* ranges employed were around 1.2–2.2 Å and 3.5–15.0 Å for Mo-C, 2.2–3.3 Å and 3.5–15.5 $Å^{-1}$ for Mo-N, and 4.2–5.3 Å and 6.5–15.5 $Å^{-1}$ for Mo-Cu, respectively. On the contrary, in the Cu *K*-edge EXAFS (typical *k* range employed in the FT was 2.8–15.3 $Å^{-1}$), weak contributions from the axial N and O atoms with longer distances should be overlapped between the first-NN Cu-N(equatorial) and the higher-NN Cu-C shells. Thus the features appearing around 1.0–3.4 Å cannot be separated. A three -or five-shell curve fitting analysis was performed for these contributions, using the *R* and *k* ranges for the fitting of 1.1–3.4 Å and 4.0–15.0 $Å^{-1}$, respectively. The Cu-Mo shell for (1) and (2) was treated as a single shell by employing the *R* and *k* ranges of 4.4–5.4 Å and 6.0–15.0 $Å^{-1}$, respectively.

The interatomic distances obtained are summarized in Tables I and II, while the coordination numbers are tabulated in Table III. Note that the errors shown in the tables are derived only from the statistical estimation in the fitting procedure, and no other contributions such as theoretical and/or

TABLE II. Interatomic distances (Å unit) from the Cu *K*-edge EXAFS analysis of (1–2).

	Cu-N(eq)	Cu-N,O(ax)	Cu-C(eq)	Cu-Mo(eq)
(1)LT	1.946(6)	2.183(39)	3.076(9)	5.201(9)
(1)PI	1.947(8)	2.197(13)	3.085(12)	5.197(20)
(2)LT	1.986(4)	2.228(11)	3.130(6)	5.270(3)
	1.949[a]	2.234[a]	3.092[a]	5.240[a]
(2)PI	1.988(5)	2.230(10)	3.133(7)	5.277(6)

[a]Reference 14.

model uncertainties are included. Examples of the curve fits are shown for the Mo-Cu and Cu-Mo shells in Fig. 4. Goodness of the curve fitting is excellent. It can be noted that the magnitudes of the EXAFS oscillations are considerably suppressed upon photoirradiation. Since the EXAFS oscillations of the photoinduced phases are still visible in the high *k* region as in the cases of the LT phases, the damping of the EXAFS amplitude is not mainly ascribed to the enhancement of the Debye-Waller factor but dominantly to the overall scale factor that normally originates from the coordination number.

Let us first discuss the interatomic distances of the structurally known compounds by comparing to the x-ray crystallographic data. The average Mo-C distances are obtained as 2.168(3) Å for (3) and 2.171(2) Å for (4), and the average Mo-N distances are 3.326(2) and 3.311(2) Å, respectively. These results are in excellent agreement with the x-ray data[15,16] in Table I. In the LT phase of (2) the obtained Mo-C and Mo-N distances of 2.159(3) and 3.310(2) Å are again in good agreement with the x-ray data.[14] From the crystal structure of (2), there exit three kinds of the Mo-Cu shells with the distances of 5.228 Å (N=2), 5.252 Å (N

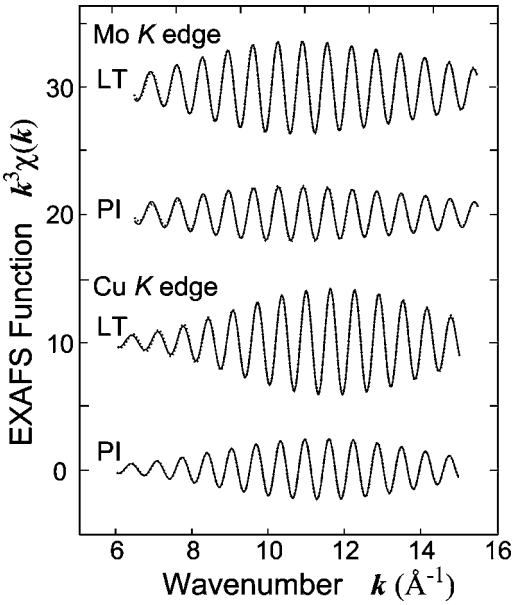

FIG. 4. Curve-fitting plots for the Mo and Cu *K*-edge EXAFS analysis of the Mo-Cu and Cu-Mo shells of (2) before (LT) and after (PI) photoirradiation.

TABLE III. Apparent coordination numbers of (1–4). The real values are 8.0 for all the Mo-C and Mo-N shells, 8.0 for the Mo-Cu shell of (1), 7.0 for the Mo-Cu shell of (2), 4.0 for all the Cu-N(eq), Cu-C(eq), and Cu-Mo shells. Values in brackets are the fixed parameters in the curve fitting due to the many-shell analysis.

Sample	Mo-C	Mo-N	Mo-Cu
(1)LT	8.3(4)	5.6(3)	2.8(3)
(1)PI	8.1(4)	4.5(3)	1.4(3)
(2)LT	8.4(4)	5.7(3)	3.5(3)
(2)PI	8.2(4)	4.3(3)	2.2(3)
(3)LT	7.9(4)	6.4(3)	
(4)LT	7.7(3)	5.8(2)	
Sample	Cu-N(eq)	Cu-C(eq)	Cu-Mo(eq)
(1)LT	4.1(3)	2.7(4)	2.1(4)
(1)PI	4.0(4)	2.5(4)	1.2(5)
(2)LT	[4.0]	[4.0]	2.4(2)
(2)PI	[4.0]	[4.0]	1.8(2)

=2), and 5.548 Å (N=4/7). Since the EXAFS analysis of the Mo-Cu shell can be done within the one-shell analysis, the longer one may not be detected, while the closer one is consistent with the EXAFS results of 5.256(4) Å. Similarly, in the Cu K-edge EXAFS analysis, the longer Cu-Mo shell is not seen. The Cu-Mo distance of (2) before photoirradiation is obtained as 5.270(3) Å (see Table II), which agrees fairly well with the Mo-Cu distance. The Cu-N distance in (2) seems a little different from that in (1): 1.946(6) and 1.986(4) Å for (1) and (2), respectively. This difference is also reflected in the Cu-Mo/Mo-Cu distances: 5.233(5) or 5.201(9) Å for (1) and 5.256(4) or 5.270(3) Å for (2). This may originate from a different environment around Cu. These results obtained indicate that the present analysis is reliable to discuss the structures of the photoinduced phases.

The estimated coordination numbers are given in Table III. As apparent in Table III, the coordination numbers of the Mo-N, Mo-Cu, and Cu-Mo shells deviate from the real values, although those of the first-NN Mo-C shells are estimated rather accurately. Especially, the deviations of the Mo-Cu and Cu-Mo shells are significant. This discrepancy can be understood in the following manner. These higher-NN shell contributions contain a strong multiple-scattering process because of the almost collinear arrangement of the Mo-C-N-Cu path. When the bond angle deviates from 180° statically or dynamically, the EXAFS amplitude is rapidly reduced. This effect cannot be described within a simple Gaussian distribution function.[22–24] We can use the effect of the amplitude reduction as a semiquantitative indicator of the bond bending.

Let us now discuss the local structures of (1) and (2) after photoirradiation. The interatomic distances do not vary compared to those before photoirradiation, as given in Tables I and II. Differences between the LT and photoinduced phases can, however, be detected in the amplitude in the EXAFS oscillation. This was already seen in the EXAFS functions $k^3\chi(k)$ or the FTs in Fig. 3. From the curve-fitting results, the coordination numbers of the Mo-N, Mo-Cu, and Cu-Mo shells are found to be reduced further compared to those before photoirradiation, while those of the Mo-C and Cu-N(eq) shells remain almost unchanged. The reduction of the EXAFS amplitude for the first-NN shells implies the enhancement of the static Debye-Waller factors. On the contrary, the (apparent) reduction of the coordination numbers for the higher-NN Mo-N, Mo-Cu, and Cu-Mo shells can be ascribed not to the breaking of the Mo-C bond but to the bending of the Mo-CN bond. The Cu-C coordination numbers in (2), however, do not vary so much upon photoirradiation. Although the curve-fitting analysis of the Cu K-edge EXAFS of (1) was conducted by fixing the coordination numbers and it is hard to recognize whether the Cu-NC bond is also bent in the photoinduced phase. We have, however, verified that when the coordination number of the Cu-C shell is assumed to be a smaller value, the resultant reliability factor becomes worse. These findings indicate that upon photoirradiation the Cu-N-C bond angles are left almost unchanged, while the Mo-C-N bond is bent.

It may ideally be possible to deduce the bent angles by performing the theoretical simulations.[18–21] In the present case, however, the photoinduced state contains both Cu(I) and Cu(II) even when the photoinduced phase transition is completed. The Cu(I):Cu(II) ratio is at most 1.0 in (1) and should be a little smaller in the present experiments. Moreover, there exist two inequivalent Cu sites in (2) and the situation is more complicated. Although we have tried to estimate the bent angles by the FEFF simulations in (2), the results should include much uncertainty and it might be better not to discuss the bent angles quantitatively.

The $Cu(NC)_4$ unit is inherently planar before photoirradiation because of the stability of the square planar structure in Cu(II), and the $Cu(NC)_4$ unit exhibits slight tetrahedral distortion after photoirradiation, which should be more stable in Cu(I). Although the present remark concerning the local structure changes in the reduction of Cu is rather qualitative, this information is essential because structural changes in the Cu redox processes have been attractive for various scientific fields. For instance, in CuZn superoxide dismutase, it is not yet settled whether Cu(I) is coordinated by three or five ligands after reduction.[25–27] Both models are based on the fact that the square planar geometry is unstable at the Cu(I) site. Although our present model may not match the case of CuZn superoxide dismutase, this model is in general worthwhile, taking into account when one wants to discuss the structural changes in the Cu redox cycle.

IV. CONCLUSIONS

In this work, we have performed the XAFS study of the photoinduced phases of the CuMo cyanides. We found direct evidence for the charge transfer phase transition from the Cu K-edge XANES: Divalent Cu is reduced to monovalent after photoirradiation. Although the changes in the interatomic distances are not found, the EXAFS results qualitatively indicate that in the photoinduced phase, the Mo-CN bond is bent while the Cu-NC bond bending is left unchanged, possibly due to slight tetrahedral distortion at the Cu(I) site.

ACKNOWLEDGMENTS

The authors acknowledge Steve Schiffman and Kristy Schiffman (University of Missouri-Rolla) for their revision of this manuscript. The authors are grateful for the financial support of the Grant-in-Aid for Scientific Research (Nos. 15201029 and 15087211) from the Ministry of Education, Culture, Sports, Science and Technology (MEXT). This work has been performed under the approval of the Photon Factory Program Advisory Committee (PF-PAC No. 2004G283).

*Electronic address: yokoyama@ims.ac.jp

[1] O. Sato, T. Iyoda, A. Fujishima, and K. Hashimoto, Science **271**, 49 (1996).
[2] A. Bleuzen, C. Lomenech, V. Escax, F. Villain, F. Varret, C. Cartier dit Moulin, and M. Verdaguer, J. Am. Chem. Soc. **122**, 6648 (2000).
[3] S. Ferlay, T. Mallah, R. Ouahès, P. Veillet, and M. Verdaguer, Nature (London) **378**, 701 (1995).
[4] S. Ohkoshi, M. Mizuno, G. J. Hung, and K. Hashimoto, J. Phys. Chem. **104**, 9365 (2000).
[5] T. Yokoyama, T. Ohta, O. Sato, and K. Hashimoto, Phys. Rev. B **58**, 8257 (1998).
[6] T. Yokoyama, M. Kiguchi, T. Ohta, O. Sato, Y. Einaga, and K. Hashimoto, Phys. Rev. B **60**, 9340 (1999).
[7] C. Cartier dit Moulin, F. Villain, A. Bleuzen, M. A. Arrio, P. Sainctavit, C. Lomenech, V. Escax, F. Baudelet, E. Dartyge, J. J. Gallet, and M. Verdaguer, J. Phys. Chem. **122**, 6653 (2000).
[8] T. Yokoyama, K. Okamoto, T. Ohta, S. Ohkoshi, and K. Hashimoto, Phys. Rev. B **65**, 064438 (2002).
[9] T. Yokoyama, H. Tokoro, S. Ohkoshi, K. Hashimoto, K. Okamoto, and T. Ohta, Phys. Rev. B **66**, 184111 (2002).
[10] S. Ohkoshi, N. Machida, Z.-J. Zhong, and K. Hashimoto, Synth. Met. **122**, 523 (2001).
[11] S. Ohkoshi, N. Machida, Y. Abe, Z.-J. Zhong, and K. Hashimoto, Chem. Lett. **2001**, 312(2001).
[12] G. Rombaut, M. Verelst, S. Golhen, L. Ouahab, C. Mathonière, and O. Kahn, Inorg. Chem. **40**, 1151 (2001).
[13] G. Rombaut, C. Mathonière, P. Guionneau, S. Golhen, L. Ouahab, M. Verelst, and P. Lecante, Inorg. Chim. Acta **326**, 27 (2001).
[14] T. Hozumi, K. Hashimoto, and S. Ohkoshi, J. Am. Chem. Soc. **127**, 3864 (2005).
[15] J. Larionova, R. Clérac, B. Donnadieu, S. Willemin, and C. Guérin, Cryst. Growth Des. **3**, 267 (2003).
[16] S. S. Basson, J. G. Leipoldt, L. D. C. Bok, J. S. van Vollenhoven, and P. J. Cilliers, Acta Crystallogr., Sect. B: Struct. Crystallogr. Cryst. Chem. **36**, 176 (1980).
[17] A. L. Ankudinov, B. Ravel, J. J. Rehr, and S. D. Conradson, Phys. Rev. B **58**, 7565 (1998).
[18] B. K. Teo, J. Am. Chem. Soc. **105**, 1144 (1983).
[19] H. I. Liu, A. Filipponi, N. Gavini, B. K. Burgess, B. Hedman, A. Di Cicco, C. R. Natoli, and K. O. Hodgson, J. Am. Chem. Soc. **116**, 2418 (1994).
[20] H. H. Zhang, A. Filipponi, A. Di Cicco, M. J. Scott, R. H. Holm, B. Hedman, and K. O. Hodgson, J. Am. Chem. Soc. **119**, 2470 (1994).
[21] M. Giorgetti, M. Berrettoni, A. Filipponi, P. J. Kulesza, and R. Marassi, Chem. Phys. Lett. **275**, 108 (1997).
[22] A. Filipponi, A. Di Cicco, and C. R. Natoli, Phys. Rev. B **52**, 15122 (1995).
[23] A. Filipponi and A. Di Cicco, Phys. Rev. B **52**, 15135 (1995).
[24] T. Yokoyama and T. Ohta, J. Phys. Soc. Jpn. **65**, 3909 (1996).
[25] W. E. Blumberg, J. Peisach, P. Eisenberger, and J. A. Fee, Biochemistry **17**, 1842 (1978).
[26] R. Osman and H. Basch, J. Am. Chem. Soc. **106**, 5710 (1984).
[27] L. M. Murphy, R. W. Strange, and S. S. Hasnain, Structure (London) **5**, 371 (1997).